Available online at www.sciencedirect.com
SCIENCE DIRECT®
Biochemical and Biophysical Research Communications 300 (2003) 65–74
BBRC
www.elsevier.com/locate/ybbrc

Choline head groups stabilize the matrix loop regions of the ATP/ADP carrier *Sc*AAC2☆

Valérie Panneels,[a,b] Ute Schüssler,[a] Sabine Costagliola,[c] and Irmgard Sinning[a,b,*]

[a] *European Molecular Biology Laboratory, 1 MeyerhofStrasse, Heidelberg 69112, Germany*
[b] *Biochemie-Zentrum Heidelberg, Universität Heidelberg, INF328, Heidelberg 69120, Germany*
[c] *Institut de Recherche Interdisciplinaire, 808 route de Lennik, Brussels 1070, Belgium*

Received 24 October 2002

Abstract

ATP/ADP carriers (AACs) are essential to the cell as they exchange ATP produced in mitochondria for cytosolic ADP. Monoclonal antibodies against the isoform 2 of *Saccharomyces cerevisiae* AAC (*Sc*AAC2) were used to probe the accessibility of the matrix loops 1 and 3 depending on the environment of the carrier. In mitochondrial membranes *Sc*AAC2 was not recognized, whereas in dodecylmaltoside the antibodies bound to the carrier, suggesting that the epitopes are hidden in the native environment. Exposure of the epitopes by detergents was reversed by reconstitution of the carrier in phospholipids or by exchanging with detergents having a choline or a trimethylammonium head group. Circular dichroism spectroscopy on peptides representing the C-terminal regions of all three matrix loops showed that only phosphocholine detergents induced a structural reorganization. Since in addition phosphatidylcholine was found to be tightly associated with the purified carrier, the matrix loop regions are likely to be associated to the membrane by phosphatidylcholine.

Keywords: ATP/ADP carrier; Antibodies; Pepscan; Phosphatidylcholine; Circular dichroism

Eukaryotic ATP/ADP carriers (AACs) play a fundamental role in supplying the cell with ATP by exchanging cytosolic ADP for ATP synthesized in the mitochondria. AACs are nuclear-encoded proteins [1,2] routed to the inner mitochondrial membrane by the TOM/TIM22 import machinery [3,4]. ATP/ADP exchange is controlled by the level of expression of the AAC isoforms [5–7] as well as by a direct modulation of the translocase activity by the membrane potential and the adenine nucleotide levels [8,9]. Three isoforms of human ATP/ADP carrier [10,11] were described whose expression is localized to the cardiac and skeletal muscles (HuAnc1/hANT1), up-regulated in proliferating cells (HuAnc3/hANT2) [6] or barely detectable in most of the tissues (HuAnc2/hANT3). A murine model of myopathy has been generated by knocking out the gene encoding the heart/muscle AAC1 isoform, which induces lactic acidosis and severe exercise intolerance [12]. The importance of AACs is also emphasized by the inability of *Saccharomyces cerevisiae* lacking the three AAC isoforms to grow on a non-fermentable medium [13]. Besides their fundamental role in the cell metabolism, AACs [14,15] and more particularly mammalian AAC1s [16] have been proposed to be involved in the apoptotic mechanism of cell death by participating in the formation of the permeability transition pore.

AACs possess six putative transmembrane domains spanning the inner mitochondrial membrane [17] which define the N- and C-terminal ends located in the intermembrane space between the two mitochondrial membranes [18] and three loops (matrix loops) located at the matrix side (Fig. 1a). Like all the members of the

☆ *Abbreviations:* AAC, ATP/ADP carrier; *Sc*AAC2, AAC isoform 2 from *Saccharomyces cerevisiae*; BA, bongkrekic acid; CATR, carboxyatractyloside; CD, circular dichroism; C12E8, octaethylene glycol monododecyl ether; CTAB, cetyltrimethylammonium bromide; DDM, *N*-dodecylmaltoside; DPC, FOS-12, phosphocholine-12; LDAO, dimethyl-dodecylamine-*N*-oxide; mAB, monoclonal antibody; PC, phosphatidylcholine; nano esi MS/MS, nano-electrospray ionization tandem mass spectrometry.

* Corresponding author. Fax: +49-6221-544790.
E-mail address: irmi.sinning@bzh.uni-heidelberg.de (I. Sinning).

0006-291X/02/$ - see front matter © 2002 Elsevier Science (USA). All rights reserved.
PII: S0006-291X(02)02795-X

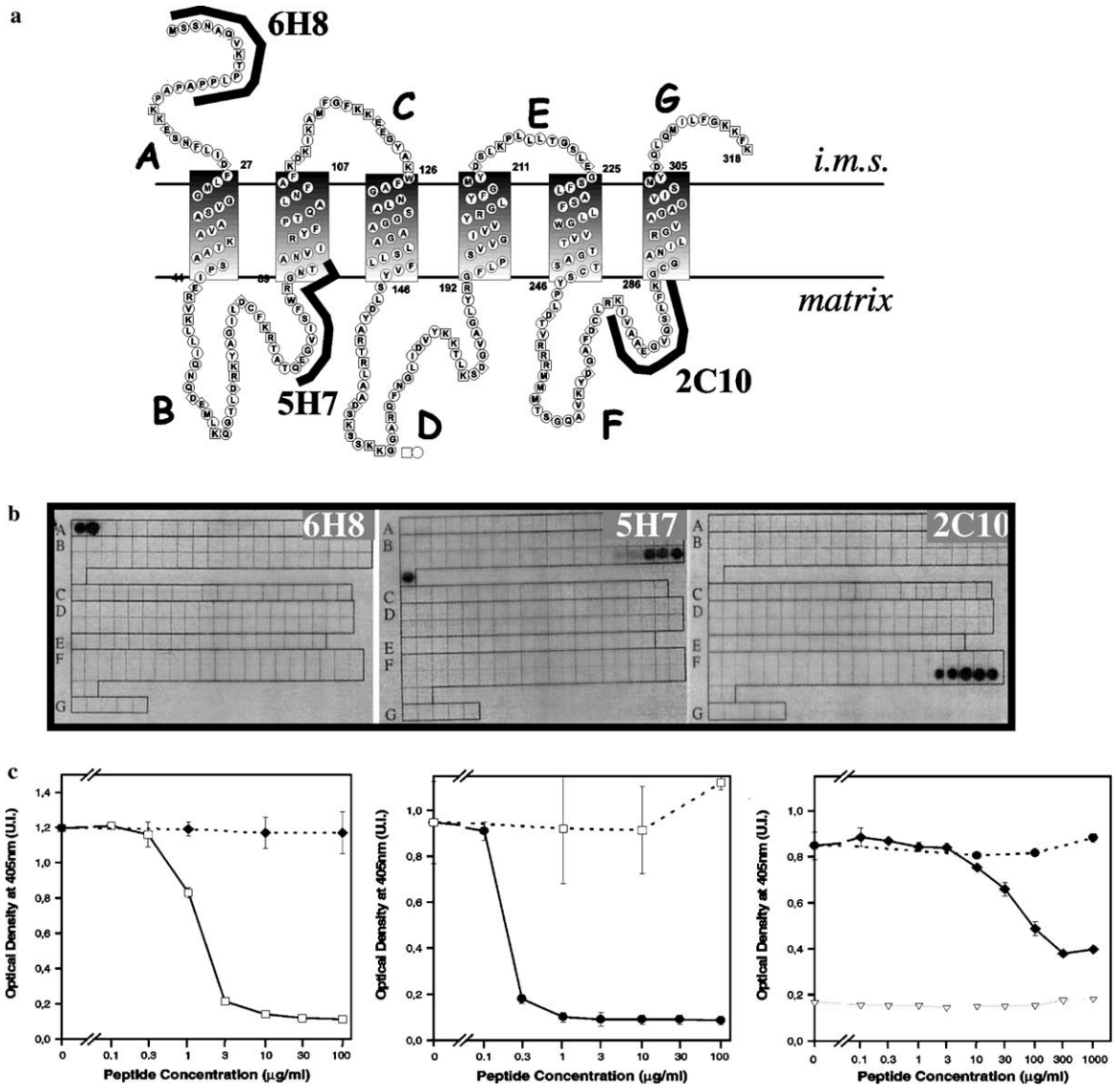

Fig. 1. Epitope mapping using a ScAAC2 peptide library and verification by peptide competition in an ELISA: (a) schematic representation of the proposed topology of ATP/ADP carrier from *S. cerevisiae* with six putative transmembrane segments (according to [53]). The N- and C-terminal ends of the carrier ('A' and 'G', respectively) and the loops 'C' and 'E' are located in the intermembrane space ('i.m.s.') of the mitochondria. The three loops B ('matrix loop 1'), D ('matrix loop 2'), and F ('matrix loop 3') are located in the matrix compartment. The location of the epitopes is indicated: 6H8, 5H7, and 2C10 mABs recognize the N-terminal cytosolic domain and the C-terminal parts of the matrix loops 1 and 3, respectively. (b) The cellulose-bound peptides covering the extramembraneous regions of *Sc*AAC2 (A–G) were incubated together with the supernatants of hybridoma cell culture of the 6H8 (left), 5H7 (middle), and 2C10 (right) mABs at a 10-fold dilution for 2 h at rt. The detection was made by chemoluminescence using a HRP-conjugated secondary antimouse antibody as described in methods. The pepscans were exposed to the autoradiographic film over a period of 1–5 s. (c) The purified *Sc*AAC2 (2 µg/ml, 100 µl) was bound to a 96-well plate and equilibrated for 10 min at rt with increasing concentrations (0, 0.1, 0.3, 1, 3, 10, 30, and 100 µg /ml) of peptides representing the epitopes as identified in (b): 6H8 □ 'SSNAQVKTPLPP,' 5H7 ● 'QEGVISFWRGN,' 2C10 ◆ 'IVAAEGVGSLFKG'; buffer: 100 µl PBS, 0.05% DDM, 300 mM NaCl, and 20 mM imidazole. The mABs 6H8 (left), 5H7 (middle), and 2C10 (right) were then added for 2 h at rt. The ELISA was developed as described in methods. A typical background signal (△) is represented in the right panel with the 2C10 peptide/2C10 mAB in the absence of *Sc*AAC2.

mitochondrial carrier family, AACs consist of a repeat of three homologous sequences of about 100 aminoacids which gives evidence for a triplication of a hypothetical common genetic precursor [1,19]. The conserved aminoacids in AACs of different isoforms and various species represent higher than 48%, suggesting a general common mechanism of nucleotide translocation. AACs are believed to work as a dimer or tetramer [20] and the expression of an active recombinant tandem-repeated dimer of *S. cerevisiae* AAC2 supports this hypothesis [21–23]. AACs exist in at least two conformations, the so-called matrix state and cytosolic state which can be stabilized by two specific inhibitors of ATP/ADP transport, bongkrekic acid (BA) and carboxyatractylo-

side (CATR), respectively. A number of observations suggest a dramatic change in the conformation of the matrix loops during the ATP/ADP exchange: chemical modifications [24–27] and proteolytic cleavage [28,29] have shown that the accessibility of some aminoacid residues of AACs in the cytosolic state is largely reduced (for a review: [2,30]). It is widely believed that some polar aminoacids of the matrix loops are even accessible from the cytosolic side of the membrane which implies that they are likely to be exposed inside the channel formed by the transmembrane domains.

In the present paper, monoclonal antibodies (mABs) against the *Sc*AAC2 were generated as tools for structural studies and the mapping of their epitopes gave new information on conformational flexibility of the carrier. ELISA and circular dichroism spectroscopy showed that two epitopes are masked in some lipid/detergent and that this inaccessibility was correlated with a change in the secondary structure of the epitopes. The natural lipids bound to the carrier were analyzed and correlated with the behavior of the epitopes in different environments. Based on our results, a model of the *Sc*AAC2 including our new data is presented.

Experimental procedures

Materials. Polyoxyethylene 10 tridecyl ether (C13E10) was purchased from Sigma Chemical (St. Louis, MO). 11-Dodecyl-β-D-maltoside (DDM), cetyltrimethylammonium bromide (CTAB), and carboxyatractyloside (CATR) were purchased from Calbiochem. *N*-Dodecylphosphocholine (FOS choline 12, DPC) and *N*,*N*-dimethyldodecylamine-*N*-oxide (LDAO) were from Anatrace and Fluka, respectively. The Ni–NTA resin and the mouse pentaHis antibody were provided by Qiagen. The secondary antibodies were purchased from Amersham or Pierce. The hydroxyapatite BioGel was purchased from Bio-Rad.

Purification of ScAAC2. Mitochondria (22–35 mg protein/ml) provided by Gérard Brandolin (Grenoble, France) were prepared [31] from the *S. cerevisiae* strain JL-1-3 [13] in which the three endogenous AAC genes are disrupted and the gene coding for the *Sc*AAC2 with a C-terminal 6histidine-tag has been integrated by homologous recombination at the *Sc*AAC2 locus [31]. *Sc*AAC2 was stabilized by an incubation of mitochondria with carboxyatractyloside at neutral pH (CATR, 20 μM) or bongkrekic acid at pH 6.5 (BA, 20 μM) for 20 min on ice. *Sc*AAC2 was purified on a hydroxyapatite column [32] followed by a Ni–NTA affinity chromatography [31]. Briefly, *Sc*AAC2-CATR or *Sc*AAC2-BA was solubilized on ice by a 5 min incubation of mitochondria with Na_2SO_4 100 mM, EDTA 1 mM, Tris 10 mM, pH 7.1, DDM 1%, C13E10 1%, and PMSF 1 mM (10 mg mitochondrial protein/ml). After a short centrifugation at 13,000*g*, the solubilized material was loaded on to the hydroxyapatite column (1 ml BioGel resin for 2 mg mitochondrial protein) and the flowthrough containing *Sc*AAC2 was collected. The fraction containing *Sc*AAC2 was then diluted five times with a DDM 0.1%, sodium phosphate buffer 50 mM, pH 7.1, and the EDTA was chelated by $MgSO_4$ 3 mM. The *Sc*AAC2 was then fixed for 45 min at 4 °C on a Ni–NTA resin in batch equilibrated with the DDM-phosphate buffer, washed three times during 10 min, and eluted directly by three volumes of imidazole 500 mM in the DDM-phosphate buffer. The purified *Sc*AAC2 was then dialyzed (MWCO 25,000 Da) against PBS, DDM 0.05% and concentrated if necessary using a Centricon 10 (Millipore). In those conditions the purified carrier is in a dimeric form (not shown).

ScAAC2 protein immunization. Six to eight week-old female Balb/c mice were immunized every 3 weeks for 2 months with the purified *Sc*AAC2 (100 μg) stabilized by CATR together with 10 μl Maalox (Rhone-Poulenc Rorer, Belgium) and 50 μl Vaxicoq (Mérieux-MSD, France) in the intraperitoneal cavity in a final volume of 200 μl PBS-DDM 0.05%. Mice positive for *Sc*AAC2 immunization were selected by ELISA screening of their sera and boosted i.v. by 50 μg *Sc*AAC2-CATR in PBS-DDM 0.05%. A classical polyethylene glycol-promoted fusion (ClonaCell-HY Kit, CellSystems) was performed between the splenic lymphocytes and the murine sp2/0 myeloma cells. Positive hybridoma cells were identified by ELISA using the purified his-tagged *Sc*AAC2 bound on Ni–NTA plates (see hereunder).

Detection of ScAAC2 by ELISA. Two hundred of purified *Sc*AAC2 in PBS with 0.05% (w/v) DDM was distributed per well in a 96-well nickel plate from Qiagen and incubated at 4 °C for 45 min. The plate was saturated with 2% BSA in PBS for 30 min at rt. For reconstitution of *Sc*AAC2 into a lipid environment, the detergent was exchanged for phospholipids (POPC–POPE–DMPA–CL (60:23:2:15), 0.5 mg/well) O/N at 4 °C in the presence of 10 mg wet Biobeads SM-2 adsorbent (Bio-Rad) in the well. The first antibody was added for 45 min at rt followed by the secondary alkaline phosphatase (AP)-conjugated antimouse antibody (Pierce, 1/1000) for another 45 min at rt. *p*-Nitrophenylphosphate substrate (Sigma) was used for detection.

Back-titration experiments [18]. Mitochondria were homogenized in glacial buffer containing 10 mM MOPS, pH 6.7, 0.12 M KCl, 1 mM EDTA, and 100 μM PMSF, the homogenate was centrifuged at 4 °C (2500*g* for 10 min), and the pellet was resuspended to 20 mg/ml in the same buffer. In some experiments the membranes were then sonicated for optimizing the presentation of the matrix side of the *Sc*AAC2 to the antibodies. Increasing quantities of mitochondrial membranes (0.3–300 μg/well) were incubated with the mAB in 150 μl PBS containing 100 μM PMSF in 96-well plates O/N at 4 °C or 60 min at rt. After incubation the plates were centrifuged at 2500*g* for 30 min at 4 °C and the supernatant (110 μl) was collected for antibody quantification. For the detergent-solubilized *Sc*AAC2, the polyhistidine-tagged carrier was bound to the resin for 45 min at 4 °C in a 50 mM phosphate buffer, pH 7, with 0.05% DDM and 100 μM PMSF. The resin was then washed and resuspended in the same buffer. Increasing quantities (0.006–6 μg/well) of pure *Sc*AAC2 bound on the Ni–NTA resin were incubated in suspension with the mAB in 150 μl phosphate-DDM buffer in 96-well plates for 60 min at rt. The plates were then centrifuged for 10 min at 3000*g* and the supernatant was collected. One hundred and ten μl supernatant collected and divided for titrating the free antibody (2×30 μl) and measuring the background (30 μl) by ELISA on a nickel plate with or without the urea-denatured *Sc*AAC2 (200 ng), respectively. The next steps of the titration assay were developed like in a classical ELISA as described in the previous section.

Epitope mapping. A peptide library [33] consisting of 179 tridecameric peptides shifted by one aminoacid representing the sequence of *Sc*AAC2 was synthesized (Jerini, Germany). The core regions of the predicted transmembrane domains were not included in the pepscan to avoid non-specific interactions which are often observed with hydrophobic peptides. The six regions corresponding to the N-terminus (M1-G31), the 5 loops (A41-N93, N104-G134, V145-S196, Y207-F231, and T238-N291) and the C-terminus (I302-K318) were labeled from A to G, respectively. The epitopes were recognized by the mABs by incubating the pepscans A to G with the culture medium of the hybridoma clones (dilution 1/10) in 0.05% Tween 20, 0.5% (w/v) low fat milk powder, 140 mM NaCl, 4 mM KCl, 50 mM Tris–HCl, pH 8 and for 2 h at rt. The HRP-conjugated antimouse secondary antibody was used at a 1/3000 dilution in the same buffer. After a classical ECL detection, the pepscans were regenerated by one or several incubations of 30 min at 50 °C in 2% (w/v) SDS, 100 mM 2-mercaptoethanol, and 50 mM Tris, pH 6.7.

Far-UV circular dichroism in various detergents. CD spectra were acquired on a Jasco-J710 spectropolarimeter calibrated with (1*S*)-(+)-

10-camphorsulfonic acid. Usually 10 scans were performed in the range 190–250 nm at a temperature of 20 °C by taking points every 0.1 nm at a 50 nm/min scan rate with an integration time of 2 s and a 1 nm bandwidth. The peptides (50 μM) were mixed with the neutral detergent polyoxyethylene ether C12E8 or DDM or with the zwitterionic detergent DPC or LDAO at a concentration at least three times above the critical micellar concentration (10 mM) in 5 mM phosphate buffer (pH 7.2). The analysis was performed after 10 min in a 0.1 cm path length cell.

Mass spectrometry of ScAAC2 phospholipids. Lipids were extracted from the purified DDM-C13E10-solubilized *Sc*AAC2 (1 mg) by Bligh and Dyer [34]. The phospholipids were separated from DDM detergent by an octadecyl preparative thin layer chromatography (Merck). Mass spectrometric analysis was performed with a triple quadrupole instrument (Finnigan-MAT (San Jose, CA) model TSQ 7000) equipped with a nanoelectrospray source [35]. The sample in $CHCl_3$:CH_3OH (1:1) was analyzed by nano-ESI-MS/MS for different classes of phospholipids (PC, PE, and CL) by either precursor ion or neutral loss scanning [35].

Results

Production of monoclonal antibodies and epitope mapping

Mice were immunized with the purified *S. cerevisiae* AAC2 (*Sc*AAC2) stabilized by the inhibitor CATR and monoclonal antibodies (mABs) were generated. The mABs 6H8, 5H7, and 2C10 were selected for their strong immunoreactivity towards the carrier in an ELISA using purified ScAAC2-6his bound on a nickel plate. All three mABs recognized the carrier in Western blot and 6H8 mAB strongly labeled the inner membrane of the yeast mitochondria in electron microscopy (not shown). The relative abundance of *Sc*AAC2 in mitochondria makes the carrier a good mitochondrial marker that can be detected by 6H8, e.g., in 2D gel electrophoresis.

A peptide library [33] corresponding to the aminoacid sequence of *Sc*AAC2 except for the very hydrophobic transmembrane domains was used for epitope mapping. The mABs were tested against the seven sub-libraries representing the predicted seven extramembranous regions (labeled A–G, Figs. 1a and b): 6H8 mAB recognized the first 13 aminoacids of *Sc*AAC2 ('MSSNAQVKTP LPP'), 5H7 the C-terminal end of the first matrix loop ('QEGVISFWRGN') and 2C10 the C-terminal end of the third matrix loop ('IVAAEGVGSLFKG'). The determination of these three different epitopes was confirmed by a competition of the mABs binding to *Sc*AAC2 with the corresponding peptides in an ELISA (Fig. 1c). All peptides competed even though 2C10 mAB had very high affinity for the carrier and the peptide could not totally compete most likely due to peptide insolubility at these high concentrations. The peptide library was also used to test the sera of nine *Sc*AAC2-immunized mice: none of them tested positive for the central matrix loop or the C-terminal end of *Sc*AAC2 (not shown). This suggests that those domains are not exposed or poorly immunogenic.

An initial Blast Search (BLASTP program, WU BLAST 2.08, EMBL server) [36] with the epitopes of the mABs in the Swiss Protein Database [37] suggested the uniqueness of the 6H8 and 2C10 epitopes. The high specificity of 6H8 and 2C10 for *Sc*AAC2 was confirmed by Western blot analysis on mammalian AACs (not shown). The 5H7 epitope ('QEGVISFWRGNTAN') shares aminoacid sequence homology with the related region of the mammalian AACs. In particular, the valine in position 4 of the epitope is conserved in all the mammalian AAC2/3 isoforms and is replaced by a phenylalanine in the mammalian AAC1 sequences. Western blot and pepscan analysis showed that 5H7 mAB recognized only the AAC2/3 isoforms and not the mammalian AAC1s (not shown). This difference in selectivity makes 5H7 mAB a potential tool for discriminating between the level of expression of AAC2/3 and AAC1 isoforms by Western blot in mammalian tissues.

Detergents/lipids influence the accessibility of the matrix loop epitopes

The mABs 6H8, 5H7, and 2C10 were tested in ELISA for their capacity to recognize the carrier in the native environment. The disadvantage of a direct ELISA is that the coating of *Sc*AAC2 to a matrix could affect its structural integrity. To avoid this possibility we performed an indirect assay, called the back-titration assay [18], in which the antibodies are first reacting with the antigen in suspension, the complexes are removed, and the free unreacted antibodies are measured. Increasing quantities of mitochondrial membranes were incubated with a constant amount of 6H8, 5H7, and 2C10 mABs and the fraction of unbound mABs left in the supernatant was titrated in an ELISA plate coated with *Sc*AAC2 denatured by urea. The 6H8 antibody recognized the native *Sc*AAC2 embedded into the mitochondrial membrane. In contrast, 5H7 and 2C10 mABs did not recognize the native carrier (Fig. 2A), even after freezing/thawing and sonication (submitochondrial particles) [38] to improve the presentation of the matrix side of *Sc*AAC2 in the assay. Back-titration ELISA was also performed with purified DDM-C13E10-solubilized *Sc*AAC2 bound to nickel resin. Under these conditions all three mABs recognized *Sc*AAC2 (Fig. 2B). The mitochondrial membranes of yeast grown in lactic acid contain about 2 μg AAC2 per 100 μg membrane (Brandolin, personal communication). A direct comparison of Figs. 2A and B led to the conclusion that even a 100-fold excess of the carrier in the membranes over the purified protein is not sufficient to promote binding of the 5H7 or 2C10 antibodies. This shows that the two epitopes in the matrix loops are exposed in DDM-C13E10-solubilized *Sc*AAC2 and hidden when *Sc*AAC2 is embedded in the mitochondrial membrane. The epitopes were inaccessible in both CATR and BA bound forms of the carrier in membranes (not shown).

To investigate if the exposure of the epitopes by detergent was reversible, the solubilized *Sc*AAC2 was

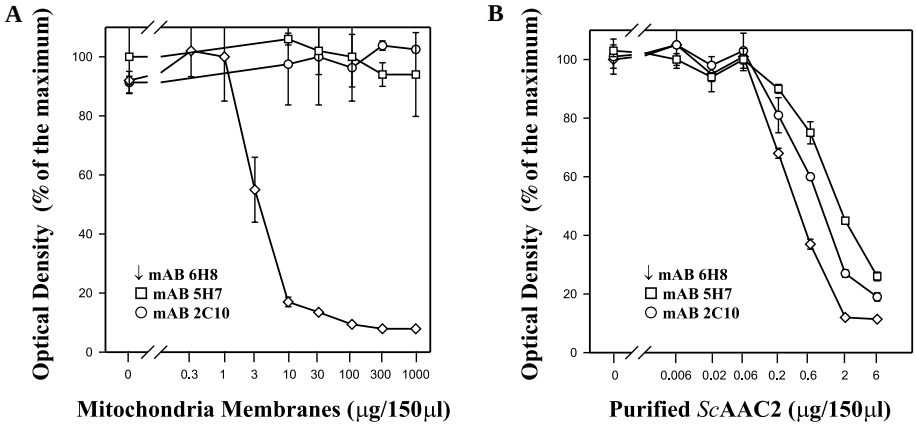

Fig. 2. Different recognition of ScAAC2 embedded in mitochondrial membranes or in the solubilized form in ELISA: (A) Increasing quantities of mitochondrial membranes (0.3–1000 μg/well) were preincubated with the 6H8 antibody (ascites, 7000-fold diluted) (◇), with the 5H7 antibody (ascites, 750-fold diluted) (□) or with the 2C10 antibody (ascites, 1000-fold diluted) (○) for 60 min at rt. The membranes were centrifuged and the supernatant containing the free unbound antibody was collected for titration. (B) Increasing quantities of purified *Sc*AAC2 (0.006–6 μg/well) bound on nickel resin were incubated with the 6H8 antibody (ascites, 7000-fold diluted) (◇), with the 5H7 antibody (ascites, 750-fold diluted) (□) or with the 2C10 antibody (ascites, 1000-fold diluted) (○) for 60 min at rt in the presence of DDM. The resin was pelleted and the supernatant was collected for titration of the unbound antibody in a classical ELISA.

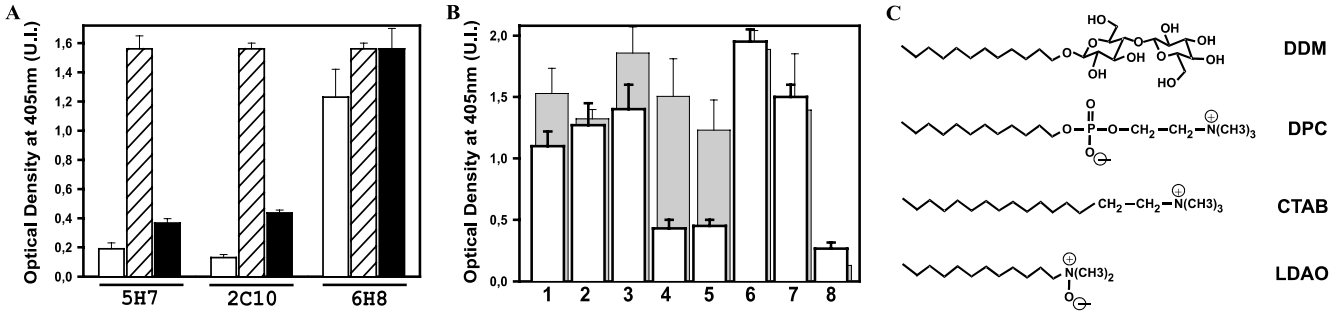

Fig. 3. Influence of choline on the exposure of 5H7 and 2C10 epitopes by ELISA. (A) Mitochondrial membranes (empty), purified *Sc*AAC2 in DDM detergent (hatched) or reconstituted in lipids (POPC–POPE–DMPA–CL (60:23:2:15), 0.5 mg per well) (black), were tested in a direct ELISA for 5H7, 2C10, or 6H8 mAB binding. (B) DDM-C13E10-solubilized *Sc*AAC2 (100 ng) was coated in a 96-well plate and subjected to a detergent exchange for 2 h at 4 °C with DDM-C13E10 (1), Triton X-100 (2), DDM (3), DPC (4), CTAB (5), LDAO (6), and CHAPS (7) at a concentration three times the cmc. 6H8 (grey), 5H7 (white), or 2C10 (not shown) mABs were then tested for recognition of the carrier by a classical ELISA. Bars "8" are the typical background values without *Sc*AAC2 (here in DDM-C13E10). (C) Structure of detergents DDM, DPC, CTAB, and LDAO.

reconstituted in a lipid environment in an ELISA. Fig. 3A shows that 5H7 and 2C10 mABs do not recognize *Sc*AAC2 reconstituted in phospholipids whereas 6H8 recognized *Sc*AAC2 in mitochondrial membrane, as well as the solubilized or the reconstituted form. Zwitterionic and neutral detergents with different polar head groups and hydrophobic chain lengths were tested to explore the influence of surface properties and micelle size on the accessibility of the epitopes. The carrier solubilized in DDM-C13E10 was coated into a 96-well plate and the detergent was then exchanged for DDM, Triton X-100, C12E8, DPC, CTAB, LDAO, or CHAPS, respectively. Fig. 3B shows that the 5H7 mAB recognized the carrier in all detergents except DPC and CTAB (Fig. 3C) whereas 6H8 recognized the carrier under all conditions. Similar results were obtained for the 2C10 mAB (not shown). The matrix antibodies did not also recognize the carrier neither after direct solubilization by DPC nor when solubilized by phosphocholine detergents with various chain lengths (10–16 carbon atoms) (not shown). The fact that 5H7 and 2C10 can discriminate between different conformations of the matrix loops makes them powerful tools for selecting a detergent for solubilization and to assess the quality of protein preparations for crystallization. Our results show that the exposure of the epitopes located in matrix loops 1 and 3 depends on the head group of the detergent and can be reversed by reconstitution into lipids.

Detergents influence the conformation of matrix loop regions

The accessibility of 5H7 and 2C10 epitopes depends on the detergent used for solubilization. The possibility of a conformational change induced by interaction with the detergent in those regions of the carrier was

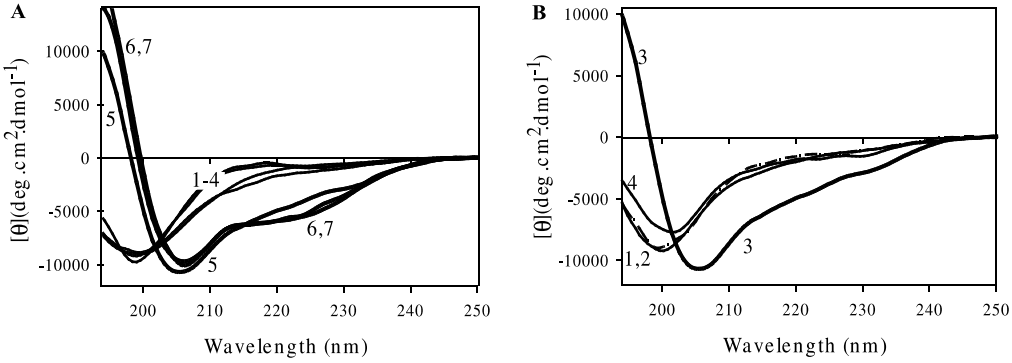

Fig. 4. Effect of detergents on the conformation of matrix loop peptides by circular dichroism. (A) CD spectra of peptides (50 μM) 5H7pep (1), 'VAGLY'pep (2), and 2C10pep (3) in the phosphate buffer. CD spectra of peptides (50 μM) 6H8pep (4), 5H7pep (5), 'VAGLY'pep (6), and 2C10pep (7) in the presence of DPC micelles (10 mM). (B) CD spectra of the 5H7peps (50 μM) in C12E8 (1), DDM (2), DPC (3), and LDAO (4). The results of the two figures were obtained by substracting the spectrum of a mixture containing all components (buffer plus detergent) but the peptide and are expressed in mean residue ellipticity.

investigated by circular dichroism spectroscopy. Peptides representing the epitopes of these two mABs were analyzed in the presence of various detergents. As the three matrix loops share sequence homology, a peptide representing the C-terminal end of the central matrix loop, the 'VAGLY' peptide 'TLKSDGVAGLYRGF,' was also included in this experiment. Fig. 4A shows that all three peptides are in random coil conformation in the phosphate buffer whereas the intense positive CD band induced by the presence of DPC (10 mM) demonstrates a profound structural organization of the peptides different from random coil conformation. The influence of CTAB could not be analyzed by CD spectroscopy due to the bromide quenching. The 6H8 peptide corresponding to the N-terminus of *Sc*AAC2 remained in a random coil conformation when mixed with DPC under the same conditions (Fig. 4A). In order to test whether other detergents, neutral or zwitterionic, can also induce a conformational change, 5H7pep was mixed with C12E8, DDM or LDAO: the spectra were typical for a random coil conformation showing that the peptide does not adopt a particular fold in these detergents (Fig. 4B). These results show that all three homologous regions of the matrix loops interact with detergent micelles and undergo a conformational change specifically with DPC which might be the reason why the 5H7 and 2C10 epitopes are masked in *Sc*AAC2 solubilized by DPC.

Analysis of the lipid content of purified ScAAC2

The 5H7 and 2C10 epitopes are masked in the native *Sc*AAC2 and their corresponding peptides interact

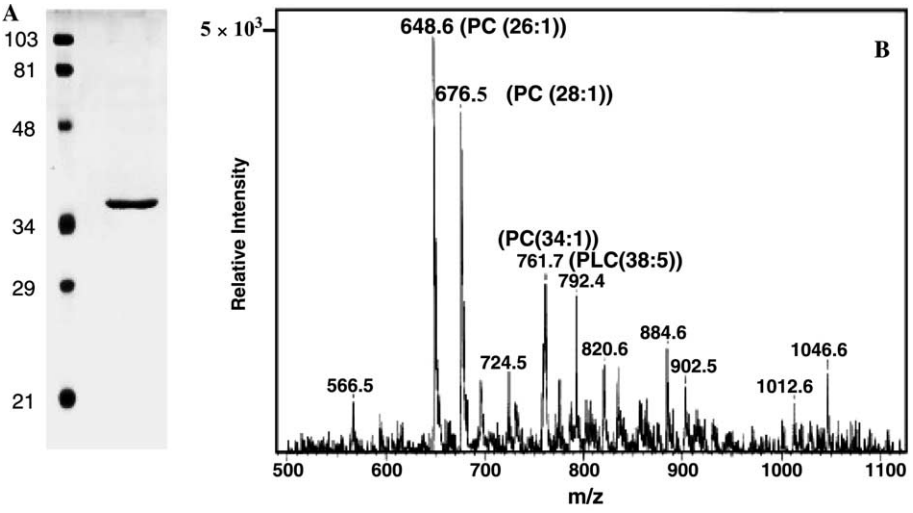

Fig. 5. ScAAC2-associated phospholipids analyzed by nano-esi-MS/MS. (A) Coomassie blue gel of the DDM-C13E10-solubilized carrier purified by nickel affinity chromatography in the presence of DDM. (B) Lipids were extracted by Bligh and Dyer from 1 mg *Sc*AAC2 and separated from the DDM detergent by octadecyl preparative TLC. Individual classes of phospholipids (PC, PE, and CL) were investigated by either precursor ion or neutral loss scanning [35]. The figure shows the specific detection of $[M + H]^+$ ions of choline species by positive ion esi-MS/MS by precursor scanning for *m/z* 184 (collision cell offset, −40 V).

preferentially with detergents with a choline head group as shown by CD analysis. This suggests that those regions of the matrix loops might be associated with phospholipids in the membrane. Therefore, the lipids associated with the purified *Sc*AAC2 (Fig. 5A) were extracted with organic solvents for lipid analysis. Individual classes of phospholipids (PC, PE, and CL) were analyzed in nano-ESI-MS/MS by either precursor ion or neutral loss scanning. Different species of phosphatidylcholines PC (26:1), (28:1), (32:1) or plasmenylcholine (38:5) were detected in small amounts (Fig. 5B), but no cardiolipin (negative ion mode, parent ion scanning for *m*/*z* 153) and no phosphatidylethanolamine (not shown) (positive ion mode, parent ion scanning for *m*/*z* 153). This shows that PC lipids bind to the carrier and that to some extent, this interaction even resists the stringent washing steps during purification.

Discussion

Monoclonal antibodies (mABs) were generated against the *Sc*AAC2 complexed with CATR and three high affinity mABs named 6H8, 5H7, and 2C10 were selected. 6H8 recognized the very first 13 N-terminal aminoacids (Fig. 1a). A number of mABs against the N-terminus were isolated from different mice. This might be explained by the fact that this region of *Sc*AAC2 is not homologous to the mouse AAC isoforms while the rest of the sequence shares a minimum of 48% sequence identity and 62% homology. The 5H7 and 2C10 epitopes are located at the C-terminal end of the matrix loops 1 and 3 (Fig. 1a), respectively, and share sequence homology. Although it was surprising to obtain antibodies against domains located so close to the transmembrane regions (predicted TMII and IV, respectively), these domains seem to be highly immunogenic. Indeed, polyclonal sera from sheep immunized against another mitochondrial carrier family member, the uncoupling protein (UCP) recognized the C-terminus of all three matrix loops [39]. In contrast, none of the mABs and sera against *Sc*AAC2 tested by pepscan recognized an epitope within the central matrix loop. Since the C-terminal parts of the three matrix loops of UCP and AACs [1] have similar polarity and share significant sequence homology one would expect that the second matrix loop of *Sc*AAC2 is immunogenic. The absence of antibodies against linear epitopes from the second matrix loop which is part of the nucleotide binding domain [40–42] suggests that this region is not accessible especially in the presence of CATR [24,28].

The 5H7 and 2C10 mABs against the predicted matrix loops 1 and 3 failed to recognize *Sc*AAC2 in mitochondrial membranes and submitochondrial particles in both the CATR and BA bound conformations. This suggests that these epitopes (see Fig. 6C) are somehow permanently associated to the membrane and not accessible when *Sc*AAC2 is embedded in a lipid environment, but are exposed and recognized in DDM. This exposure of the epitopes during solubilization is reversible since reconstitution of the purified *Sc*AAC2 into a lipid environment led to a loss of recognition by 5H7 and 2C10 mABs. Different classes of detergents were tested for their capacity to mask the epitopes. DPC contains a zwitterionic phosphocholine head group, CTAB is a cationic detergent with an ammonium group but no phosphate, LDAO a zwitterionic detergent with a N-oxide group and DDM is neutral with a maltoside head group (see Fig. 3C). DPC and CTAB were the only detergents able to mask the epitopes and thus mimic the lipid environment. This shows that the head group is important and an ammonium group is required but not a phosphate group. Change in the chain length of phosphocholine detergents had no influence on the exposure of the epitopes, which shows that the head group rather than the size of the micelle [43] is critical.

From those experiments we reasoned that a specific interaction of DPC with the regions of *Sc*AAC2 corresponding to the epitopes could induce a structural reorganization of those regions. We used CD spectroscopy to study the influence of the same detergents on the conformation of peptides corresponding to the C-terminal ends of all three matrix loops. DPC induced a dramatic structural rearrangement of all three peptides. In the detergents C12E8, DDM, and LDAO the peptides could not adopt a specific fold and remained in a random coil conformation. The specificity of DPC to induce a conformational change of the peptides supports the hypothesis that the epitopes in *Sc*AAC2 are masked due to an interaction with the choline head groups. As all three peptides contain a negatively charged residue (glutamate, aspartate) and an aromatic residue (tryptophane, tyrosine, and phenylalanine in the loops 1–3), the interaction with a positively charged amine might occur via an ionic or a π–cation interaction [44], respectively.

Dodecylphosphocholine (DPC) is structurally related to phosphatidylcholine lipids (PCs) and was found by NMR relaxation experiments to mimic 'a membrane-like environment' [45]. Previously, PC was used in translocation assays of the ATP/ADP carrier in order to prevent leakage of the vesicles and cardiolipin was reported to be essential for the nucleotide translocation [46]. Lipid analysis by mass spectrometry presented here shows that PCs with different chain lengths, saturated or unsaturated, remain bound to *Sc*AAC2 even after extensive washing during nickel affinity purification. This indicates a specific association of PC with the ATP/ADP carrier. Under these conditions, a proportion of 5H7 and 2C10 epitopes of the purified AAC are exposed and PC lipids remain most likely bound to the central matrix loop stabilized by CATR. Since cardiolipin was not detected the binding must be weaker. The role of

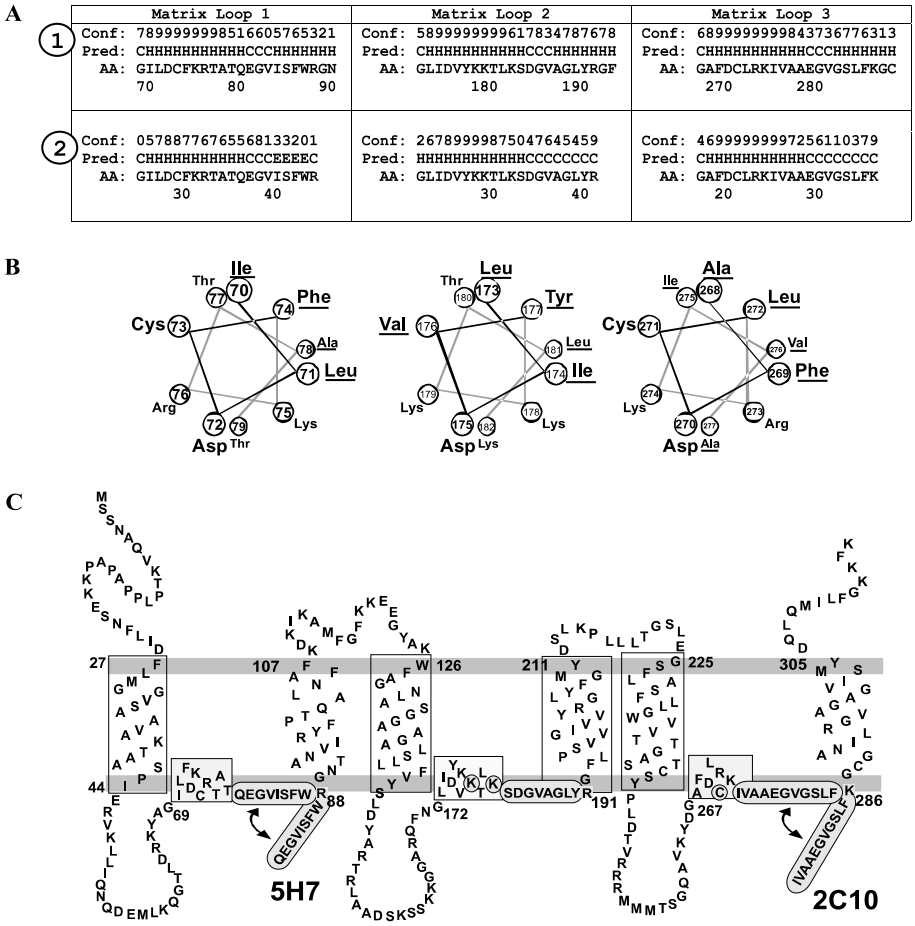

Fig. 6. Proposed model of the secondary structure of ScAAC2 in the presence of phosphatidylcholine. (A) Secondary structure prediction results by the PSIPRED software on the full-length carrier (1) or the isolated matrix loops (2). The prediction results on the last half part of each matrix loops are shown. The nomenclature E, H, C represents respectively the prediction of strand, helix or coil secondary structure. The confidence ('Conf') is scored with a highest probability of 9. (B) Helical wheel depiction of the regions of each matrix loop predicted to form an amphipathic α-helix: the 'ILDCFKRTAT' peptide (left), the 'LIDVYKKTLK' peptide (middle), and the 'AFDCLRKIVA' peptide (right) from the matrix loops 1, 2, and 3, repectively. The hydrophobic residues are underlined. (C) Model of the *Sc*AAC2 with the six predicted transmembrane domains, the three amphipathic domains in a light grey box, and the 5H7 and 2C10 epitopes (dark grey box) associated to the membrane. The aminoacid residues K179, K182, and C271 are marked.

cardiolipin might be to buffer positive charges in the nucleotide binding site and attenuate the affinity for the negatively charged ligand in order to allow reversibility of nucleotide binding. This would facilitate the release of ADP in the matrix compartment. A similar role was already proposed for the mechanism of release of ADP from the ATP binding site of the DnaA protein in *Escherichia coli* [47,48]. This might suggest that PC stabilizes the structure of matrix loops whereas cardiolipin is required for translocation of the nucleotide [49].

Two lysines of *Sc*AAC2 (K179, K182) have been identified as key residues for the cardiolipin-dependent nucleotide transport and their interaction with cardiolipin implies that they are in close proximity to the membrane [50]. In addition, chemical modifications of cysteines of matrix loops 2 and 3 in the bovine carrier which are just upstream of the 'VAGLY' and 2C10 peptides, respectively, showed that those regions are likely hidden in the membrane [26]. Together with those data and in accordance with our results, this suggests that the 5H7 and 2C10 epitopes are included in a larger domain associated to the membrane. A secondary structure analysis on the three matrix loops of ScAAC2 using the PSIPRED software predicted the presence of short α-helices upstream of the 5H7 and 2C10 epitopes and the 'VAGLY' peptide (Fig. 6A). The same predictions were found by the PHD program [51]. In a helical wheel depiction, these regions show a distribution of polar and hydrophobic aminoacids which is in agreement with an amphipathic α-helix (Fig. 6B). The three regions all contain positively charged residues. A detailed topology study on lysine-containing amphipathic peptides [52] suggests that the number of lysine residues is important for membrane insertion or association. Increasing the number of lysines decreases the capacity of a peptide to insert into the membrane. Interestingly,

the central matrix loop contains three lysines in the amphipathic helix (see Fig. 6C). Taken together these data suggest that the C-terminal regions of the three matrix loops are associated with the membrane. The N-terminal regions of each matrix loops contain the flexible regions in which the aminoacids K59, K164, and K264 change accessibility from the BA to the CATR conformation [28,29]. The flexible and membrane-associated regions of the matrix loops are separated by a glycine (G69 and G172 are strictly conserved in AACs, G267 is partially conserved) which might act as a hinge between these two regions. Taken together, our data suggest that the matrix loops contain distinct regions of different flexibilities. Whereas the aminoterminal regions of the matrix loops have been shown to be accessible in the BA form of the carrier, the C-terminal regions are always anchored to the membrane irrespective of the presence of inhibitors and are only exposed when the protein is not in the correct environment.

Acknowledgments

We thank Gérard Brandolin (CEA, Grenoble) and his group for helpful discussions and for the preparation of mitochondria. We thank Manoli de la Paz (EMBL, Heidelberg) for helpful discussions on the CD analysis. We thank Wolf Lehmann (dkfz, Heidelberg) for the nano-ESI-MS/MS analysis. We thank Stefan Dübel, Joachim Koch, and Çagla Eroglu for helpful discussions. Sabine Costagliola is *Chercheur Qualifié* at the *Fond National de la Recherche Scientifique* (FNRS, Belgium). Valérie Panneels was supported by the BIO4-CT-972119 network grant to I.S.

References

[1] J. Kuan, M.H.J. Saier, The mitochondrial carrier family of transport proteins: structural, functional, and evolutionary relationships, Crit. Rev. Biochem. Mol. Biol. 28 (1993) 209–233.
[2] C. Fiore, V. Trezeguet, A. Le Saux, P. Roux, C. Schwimmer, A.C. Dianoux, F. Noel, G.J. Lauquin, G. Brandolin, P.V. Vignais, The mitochondrial ADP/ATP carrier: structural, physiological and pathological aspects, Biochimie 80 (1998) 137–150.
[3] M. Endres, W. Neupert, M. Brunner, Transport of the ADP/ATP carrier of mitochondria from the TOM complex to the TIM22.54 complex, EMBO J. 18 (1999) 3214–3221.
[4] J. Rassow, P.J.T. Dekker, S. van Wilpe, M. Meijer, J. Soll, The preprotein translocase of the mitochondrial inner membrane: function and evolution, J. Mol. Biol. 286 (1999) 105–120.
[5] G. Stepien, A. Torroni, A.B. Chung, J.A. Hodge, D.C. Wallace, Differential expression of adenine nucleotide translocator isoforms in mammalian tissues and during muscle cell differentiation, J. Biol. Chem. 267 (1992) 14592–14597.
[6] S. Giraud, C. Bonod-Bidaud, M. Wesolowski-Louvel, G. Stepien, Expression of human ANT2 gene in highly proliferative cells: GRBOX, a new transcriptional element, is involved in the regulation of glycolytic ATP import into mitochondria, J. Mol. Biol. 281 (1998) 409–418.
[7] B. Sokolikova, L. Sabova, I. Kissova, J. Kolarov, A carbon-source-responsive element is required for regulation of the hypoxic ADP/ATP carrier (AAC3) isoform in *Saccharomyces cerevisiae*, Biochem. J. 352 Pt 3 (2000) 893–898.
[8] R. Kramer, M. Klingenberg, Modulation of the reconstituted adenine nucleotide exchange by membrane potential, Biochemistry 19 (1980) 556–560.
[9] T. Gropp, N. Brustovetsky, M. Klingenberg, V. Muller, K. Fendler, E. Bamberg, Kinetics of electrogenic transport by the ADP/ATP carrier, Biophys. J. 77 (1999) 714–726.
[10] A.L. Cozens, M.J. Runswick, J.E. Walker, DNA sequences of two expressed nuclear genes for human mitochondrial ADP/ATP translocase, J. Mol. Biol. 206 (1989) 261–280.
[11] D.H. Ku, J. Kagan, S.T. Chen, C.D. Chang, R. Baserga, J. Wurzel, The human fibroblast adenine nucleotide translocator gene. Molecular cloning and sequence, J. Biol. Chem. 265 (1990) 16060–16063.
[12] B.H. Graham, K.G. Waymire, B. Cottrell, I.A. Trounce, G.R. MacGregor, D.C. Wallace, A mouse model for mitochondrial myopathy and cardiomyopathy resulting from a deficiency in the heart/muscle isoform of the adenine nucleotide translocator, Nat. Genet. 16 (1997) 226–234.
[13] T. Drgon, L. Sabova, N. Nelson, J. Kolarov, ADP/ATP translocator is essential only for anaerobic growth of yeast *Saccharomyces cerevisiae*, FEBS Lett. 289 (1991) 159–162.
[14] I. Marzo, C. Brenner, N. Zamzami, J.M. Jurgensmeier, S.A. Susin, H.L. Vieira, M.C. Prevost, Z. Xie, S. Matsuyama, J.C. Reed, G. Kroemer, Bax and adenine nucleotide translocator cooperate in the mitochondrial control of apoptosis, Science 281 (1998) 2027–2031.
[15] J.C. Martinou, Apoptosis. Key to the mitochondrial gate [news; comment], Nature 399 (1999) 411–412.
[16] M.K. Bauer, A. Schubert, O. Rocks, S. Grimm, Adenine nucleotide translocase-1, a component of the permeability transition pore, can dominantly induce apoptosis, J. Cell Biol. 147 (1999) 1493–1502.
[17] M. Saraste, J.E. Walker, Internal sequence repeats and the path of polypeptide in mitochondrial ADP/ATP translocase, FEBS Lett. 144 (1982) 250–254.
[18] G. Brandolin, F. Boulay, P. Dalbon, P.V. Vignais, Orientation of the N-terminal region of the membrane-bound ADP/ATP carrier protein explored by antipeptide antibodies and an arginine-specific endoprotease. Evidence that the accessibility of the N-terminal residues depends on the conformational state of the carrier, Biochemistry 28 (1989) 1093–1100.
[19] J.E. Walker, M.J. Runswick, The mitochondrial transport protein superfamily, J. Bioenerg. Biomembr. 25 (1993) 435–446.
[20] H. Hackenberg, M. Klingenberg, Molecular weight and hydrodynamic parameters of the adenosine 5′-diphosphate–adenosine 5′-triphosphate carrier in Triton X-100, Biochemistry 19 (1980) 548–555.
[21] T. Hatanaka, M. Hashimoto, E. Majima, Y. Shinohara, H. Terada, Functional expression of the tandem-repeated homodimer of the mitochondrial ADP/ATP carrier in *Saccharomyces cerevisiae*, Biochem. Biophys. Res. Commun. 262 (1999) 726–730.
[22] V. Trezeguet, A. Le Saux, C. David, C. Gourdet, C. Fiore, A. Dianoux, G. Brandolin, G.J. Lauquin, A covalent tandem dimer of the mitochondrial ADP/ATP carrier is functional in vivo, Biochim. Biophys. Acta 1457 (2000) 81–93.
[23] S.G. Huang, S. Odoy, M. Klingenberg, Chimers of two fused ADP/ATP carrier monomers indicate a single channel for ADP/ATP transport, Arch. Biochem. Biophys. 394 (2001) 67–75.
[24] M. Klingenberg, M. Appel, Is there a binding center in the ADP, ATP carrier for substrate and inhibitors? Amino acid reagents and the mechanism of the ADP, ATP translocator, FEBS Lett. 119 (1980) 195–199.
[25] F. Boulay, P.V. Vignais, Localization of the *N*-ethylmaleimide reactive cysteine in the beef heart mitochondrial ADP/ATP carrier protein, Biochemistry 23 (1984) 4807–4812.
[26] E. Majima, H. Koike, Y.M. Hong, Y. Shinohara, H. Terada, Characterization of cysteine residues of mitochondrial ADP/ATP

carrier with the SH-reagents eosin 5-maleimide and *N*-ethylmaleimide, J. Biol. Chem. 268 (1993) 22181–22187.
[27] E. Majima, Y. Shinohara, N. Yamaguchi, Y.M. Hong, H. Terada, Importance of loops of mitochondrial ADP/ATP carrier for its transport activity deduced from reactivities of its cysteine residues with the sulfhydryl reagent eosin-5-maleimide, Biochemistry 33 (1994) 9530–9536.
[28] I. Marty, G. Brandolin, J. Gagnon, R. Brasseur, P.V. Vignais, Topography of the membrane-bound ADP/ATP carrier assessed by enzymatic proteolysis, Biochemistry 31 (1992) 4058–4065.
[29] G. Brandolin, A. Le Saux, V. Trezeguet, G.J. Lauquin, P.V. Vignais, Chemical, immunological, enzymatic, and genetic approaches to studying the arrangement of the peptide chain of the ADP/ATP carrier in the mitochondrial membrane, J. Bioenerg. Biomembr. 25 (1993) 459–472.
[30] M. Klingenberg, Molecular aspects of the adenine nucleotide carrier from mitochondria, Arch. Biochem. Biophys. 270 (1989) 1–14.
[31] C. Fiore, V. Trezeguet, P. Roux, A. Le Saux, F. Noel, C. Schwimmer, D. Arlot, A.C. Dianoux, G.J. Lauquin, G. Brandolin, Purification of histidine-tagged mitochondrial ADP/ATP carrier: influence of the conformational states of the C-terminal region, Protein Expr. Purif. 19 (2000) 57–65.
[32] M. Klingenberg, E. Winkler, S. Huang, ADP/ATP carrier and uncoupling protein, Methods Enzymol. 260 (1995) 369–389.
[33] A. Kramer, J. Schneider-Mergener, Synthesis and screening of peptide libraries on continuous cellulose membrane supports, Methods Mol. Biol. 87 (1998) 25–39.
[34] E.G. Bligh, W.J. Dyer, A rapid method of total lipid extraction and purification, Can. J. Biochem. Physiol. 37 (1959) 911–917.
[35] B. Brugger, G. Erben, R. Sandhoff, F.T. Wieland, W.D. Lehmann, Quantitative analysis of biological membrane lipids at the low picomole level by nano-electrospray ionization tandem mass spectrometry, Proc. Natl. Acad. Sci. USA 94 (1997) 2339–2344.
[36] S.F. Altschul, W. Gish, W. Miller, E.W. Myers, D.J. Lipman, Basic local alignment search tool, J. Mol. Biol. 215 (1990) 403–410.
[37] A. Bairoch, R. Apweiler, The SWISS-PROT protein sequence database and its supplement TrEMBL in 2000, Nucleic Acids Res. 28 (2000) 45–48.
[38] G. Lauquin, C. Villiers, J.W. Michejda, L.V. Hryniewiecka, P.V. Vignais, Adenine nucleotide transport in sonic submitochondrial particles. Kinetic properties and binding of specific inhibitors, Biochem. Biophys. Acta 460 (1977) 331–345.
[39] B. Miroux, V. Frossard, S. Raimbault, D. Ricquier, F. Bouillaud, The topology of the brown adipose tissue mitochondrial uncoupling protein determined with antibodies against its antigenic sites revealed by a library of fusion proteins, EMBO J. 12 (1993) 3739–3745.
[40] M.R. Block, F. Boulay, G. Brandolin, G.J. Lauquin, P.V. Vignais, Chemical modifications and active site labeling of the mitochondrial ADP/ATP carrier, Methods Enzymol. 125 (1986) 658–670.
[41] P. Mayinger, E. Winkler, M. Klingenberg, The ADP/ATP carrier from yeast (AAC-2) is uniquely suited for the assignment of the binding center by photoaffinity labeling, FEBS Lett. 244 (1989) 421–426.
[42] A.C. Dianoux, F. Noel, C. Fiore, V. Trezeguet, S. Kieffer, M. Jaquinod, G.J. Lauquin, G. Brandolin, Two distinct regions of the yeast mitochondrial ADP/ATP carrier are photolabeled by a new ADP analogue: 2-azido-3′-*O*-naphthoyl-[β-^{32}P]ADP. Identification of the binding segments by mass spectrometry, Biochemistry 39 (2000) 11477–11487.
[43] M. le Maire, P. Champeil, J.V. Moller, Interaction of membrane proteins and lipids with solubilizing detergents, Biochim. Biophys. Acta 1508 (2000) 86–111.
[44] D.A. Dougherty, Cation–π interactions in chemistry and biology: a new view of benzene, Phe, Tyr, and Trp, Science 271 (1996) 163–168.
[45] V. Beswick, R. Guerois, F. Cordier-Ochsenbein, Y.M. Coic, H.D. Tam, J. Tostain, J.P. Noel, A. Sanson, J.M. Neumann, Dodecylphosphocholine micelles as a membrane-like environment: new results from NMR relaxation and paramagnetic relaxation enhancement analysis, Eur. Biophys. J. 28 (1999) 48–58.
[46] N. Brustovetsky, A. Becker, M. Klingenberg, E. Bamberg, Electrical currents associated with nucleotide transport by the reconstituted mitochondrial ADP/ATP carrier, Proc. Natl. Acad. Sci. USA 93 (1996) 664–668.
[47] K. Sekimizu, A. Kornberg, Cardiolipin activation of DnaA protein, the initiation protein of replication in *Escherichia coli*, J. Biol. Chem. 263 (1988) 7131–7135.
[48] M. Makise, S. Mima, T. Tsuchiya, T. Mizushima, Identification of amino acids involved in the functional interaction between DnaA protein and acidic phospholipids, J. Biol. Chem. 275 (2000) 4513–4518.
[49] B. Hoffmann, A. Stockl, M. Schlame, K. Beyer, M. Klingenberg, The reconstituted ADP/ATP carrier activity has an absolute requirement for cardiolipin as shown in cysteine mutants, J. Biol. Chem. 269 (1994) 1940–1944.
[50] M. Klingenberg, D.R. Nelson, Structure–function relationships of the ADP/ATP carrier, Biochim. Biophys. Acta 1187 (1994) 241–244.
[51] B. Rost, PHD: predicting one-dimensional protein structure by profile-based neural networks, Methods Enzymol. 266 (1996) 525–539.
[52] B. Vogt, P. Ducarme, S. Schinzel, R. Brasseur, B. Bechinger, The topology of lysine-containing amphipathic peptides in bilayers by circular dichroism, solid-state NMR, and molecular modeling, Biophys. J. 79 (2000) 2644–2656.
[53] V. Muller, D. Heidkamper, D.R. Nelson, M. Klingenberg, Mutagenesis of some positive and negative residues occurring in repeat triad residues in the ADP/ATP carrier from yeast, Biochemistry 36 (1997) 16008–16018.